

# Vapor-Phase Synthesis of Mesoporous Silica Thin Films

Norikazu Nishiyama,<sup>\*,†</sup> Shunsuke Tanaka,<sup>†</sup> Yasuyuki Egashira,<sup>†</sup>  
Yoshiaki Oku,<sup>‡</sup> and Korekazu Ueyama<sup>†</sup>

Division of Chemical Engineering, Graduate School of Engineering Science, Osaka University,  
1-3 Machikaneyama, Toyonaka, Osaka 560-8531, Japan, and MIRAI Project, Association of  
Super-Advanced Electronics Technology (ASET), AIST, Tsukuba West 7, 16-1 Onogawa,  
Tsukuba, Ibaraki 305-8569, Japan

Received October 14, 2002. Revised Manuscript Received December 18, 2002

Nano-phase transition of an organic–inorganic nanocomposite under vapor infiltration of tetraethoxysilane (TEOS) or tetramethoxysilane (TMOS) was found in mesoporous thin film preparation. The rearrangement into a hexagonal periodic structure implies high mobility of the surfactant–silicate composites in solid phase. The swelling of film thickness and *d* spacing was observed under vapor infiltration. The nano-phase transition under vapor infiltration contains two competitive processes: (1) the penetration of TEOS or TMOS into the film and (2) the reaction of the silanol group. Film thickness and *d* spacing were controlled by changing synthetic temperature, silica sources (TEOS and TMOS), catalysts (HCl and NH<sub>3</sub>), and the thickness of surfactant films. The films prepared from vapor phase show superior characteristics, such as high structural stability and high resistance to water adsorption. The vapor infiltration method is a simpler process than conventional sol–gel techniques and attractive for mass production of a variety of organic–inorganic composite materials and inorganic porous films.

## Introduction

Preparation of inorganic mesoporous films has attracted considerable attention because of their possible use in membrane separations, chemical sensors, optical devices, and electronic devices such as low-*k* dielectric films. MCM-41 type mesoporous silica materials<sup>1</sup> and mesoporous silica films<sup>2–17</sup> have conventionally been

fabricated by deposition of surfactant–silicate composites from a liquid phase under acidic or basic conditions. Self-supporting thin films made of mesoporous materials with unidimensional pore structures have been prepared at air/water<sup>2–4</sup> and oil/water<sup>5</sup> interfaces. Then, supported mesoporous silica films have been reported by several research groups.<sup>6–17</sup> The mesoporous silica films were grown under acidic conditions at a variety of interfaces, including water/mica,<sup>6,7</sup> water/graphite<sup>6,8</sup> and water/silica<sup>6</sup>, by hydrothermal synthesis. A simpler way to synthesize mesoporous silica films has been developed by spin-coating<sup>9–12</sup> and dip-coating<sup>13,14</sup> methods. These solvent-evaporation techniques have been utilized for coating on glass substrates<sup>9–11</sup> and on silicon wafers.<sup>12–14</sup> We previously reported that the structural stability of spin-on mesoporous silica film was enhanced by a vapor infiltration technique using tetraethoxysilane (TEOS).<sup>15</sup>

Here we report a novel synthesis route of thin films made of periodic mesoporous silica, which is prepared from vapor phase using TEOS or tetramethoxysilane (TMOS) under acidic or basic conditions.

The mesoporous films with low concentration of silanol groups may be obtained by vapor-phase synthesis because the films are synthesized at relatively high temperature in the absence of aqueous solutions. Furthermore, from the point of view of commercialization, spin-coating solutions should be stable in the long term. In this preparation, the starting solution does not

\* Corresponding author. Phone/fax: +81-6-6850-6256. E-mail: nishiyama@cheng.es.osaka-u.ac.jp.

<sup>†</sup> Osaka University.

<sup>‡</sup> MIRAI Project.

(1) Kresge, C. T.; Leonowicz, M. E.; Roth, W. J.; Vartuli, J. C.; Beck, J. S. *Nature* **1992**, *359*, 710.

(2) Yang, H.; Coombs, N.; Sokolov, I.; Ozin, G. A. *Nature* **1996**, *381*, 589.

(3) Ryoo, R.; Ko, C. H.; Cho, S. J.; Kim, J. M. *J. Phys. Chem. B* **1997**, *101*, 10610.

(4) Schacht, S.; Huo, Q.; Voigt-Martin, I. G.; Stucky, G. D.; Schuth, F. *Science* **1996**, *273*, 768.

(5) Brown, A. S.; Holt, S. A.; Dam, T.; Trau, M.; White, J. W. *Langmuir* **1997**, *13*, 6363.

(6) Aksay, I. A.; Trau, M.; Manne, S.; Honma, I.; Yao, N.; Zhou, L.; Fenter, P.; Eisenberger, P. M.; Gruner, S. M. *Science* **1996**, *273*, 892.

(7) Yang, H.; Kuperman, A.; Coombs, N.; Mamich-Afara, S.; Ozin, G. A. *Nature* **1996**, *379*, 703.

(8) Yang, H.; Coombs, N.; Sokolov, I.; Ozin, G. A. *J. Mater. Chem.* **1997**, *7*, 1285.

(9) Ogawa, M. *J. Chem. Soc. Chem. Commun.* **1996**, 1149.

(10) Ogawa, M.; Masukawa, N. *Microporous Mesoporous Mater.* **2000**, *38*, 35.

(11) Miyata, H.; Kuroda, K. *Chem. Mater.* **1999**, *11*, 1609.

(12) Bruinsma, P. J.; Hess, N. J.; Bontha, J. R.; Liu, J.; Baskaran, S. In *Proceedings of the MRS Symposium on Low Dielectric Constant Materials II*; Materials Research Society: Pittsburgh, PA, 1997; p 105.

(13) Lu, Y.; Ganguli, R.; Drewien, C. A.; Anderson, M. T.; Brinker, C. J.; Gong, W.; Guo, Y.; Soye, H.; Dunn, B.; Huang, M. H.; Zink, J. I. *Nature* **1997**, *389*, 364.

(14) Sellinger, A.; Weiss, P. R.; Nguyen, A.; Lu, Y.; Assink, R. A.; Gong, W.; Brinker, C. J. *Nature* **1998**, *394*, 256.

(15) Nishiyama, N.; Tanaka, S.; Egashira, Y.; Oku, Y.; Ueyama, K. *Chem. Mater.* **2002**, *14*, 4229.

(16) Park, D.-H.; Nishiyama, N.; Egashira, Y.; Ueyama, K. *Ind. Eng. Chem. Res.* **2001**, *40*, 6105.

(17) Hillhouse, H. W.; van Egmond, J. W.; Tspatis, M.; Hanson, J. C.; Larese, J. Z. *Microporous Mesoporous Mater.* **2001**, *44–45*, 639.

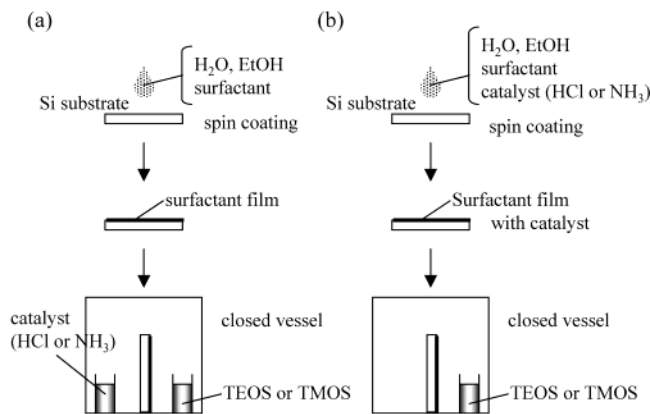


**Figure 1.** Vapor-phase synthesis of mesoporous silica films: (a) the catalyst source is from the bottom of the vessel as a vapor, (b) the catalyst is incorporated into the spinning solution.

contain silicate species which may be polymerized gradually. The vapor-phase synthesis is a simpler process than conventional sol-gel techniques and attractive for mass production of a variety of organic-inorganic composite materials and inorganic porous films.

In this paper, we show the formation of mesoporous silica film on a Si substrate under TEOS or TMOS vapor. We have studied the effect of the synthetic temperature, the film thickness of surfactant films, and the source of vapors (TEOS or TMOS, and HCl or NH<sub>3</sub>) on the structure of mesoporous silica films.

### Experimental Section

The preparation procedure for the mesoporous silica films is shown in Figure 1(a). The surfactant molecules were deposited on a silicon substrate by a spin-coating method. The precursor solution was prepared using cetyltrimethylammonium bromide (CTAB), ethanol, and/or deionized water with the mole ratios of 0.5:50:100 CTAB/EtOH/H<sub>2</sub>O. A silicon wafer was cut into 2 cm × 2 cm pieces and used as a substrate. The surfactant-solvent mixture was dropped onto the silicon substrate while it was spinning at 500 rpm, and then the substrate spun up to 1000–6000 rpm for 1 min. The surfactant-coated silicon substrate was arranged to lie vertically in a closed vessel (50 cm<sup>3</sup>). Small amounts of a silica source (TEOS or TMOS) and a catalyst (ammonia solution (1 N) or HCl (5 N)) were separately placed in the bottom of the vessel apart from the substrate. The vessel was placed in an oven at 90–180 °C for 0–12 h. The surfactant film was exposed to a saturated TEOS or TMOS vapor with an autogenous pressure. A calcination was performed at 400 °C in air for 5 h with a heating rate of 1 °C/min.

Another preparation procedure is shown in Figure 1(b). A catalyst (ammonium solution or HCl) is contained in a spin-coating solution. A vapor treatment is performed only with TEOS or TMOS. In this report, we show the synthetic results obtained using the preparation procedure (a). The results for the procedure (b) will be reported in the future.

X-ray diffraction patterns (XRD) of mesostructured films were recorded on a Rigaku Mini-Flex using CuKα radiation with  $\lambda = 1.5418$  Å in  $\theta$ - $2\theta$  scan mode. Fourier transform infrared (FTIR) spectra of mesostructured films were recorded on a FTIR-8200PC spectrometer (Shimadzu Co.) at 4 cm<sup>-1</sup> resolutions. Field emission scanning electron microscope (FE-SEM) images were recorded on a Hitachi S-5000L microscope at an acceleration voltage of 18 kV. Scanning transmission electron microscope (STEM) observation was conducted on a Hitachi HD2000 microscope operating at 200 kV.

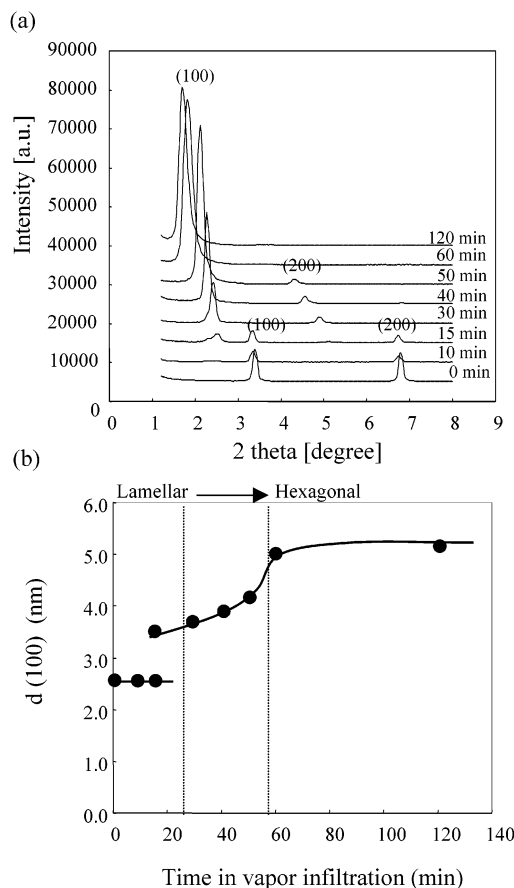


**Figure 2.** Nano-phase transition of a silica-surfactant film under vapor infiltration. (a) Time course of XRD pattern of a silica-surfactant film. (b) Change in the  $d(100)$  spacing of a mesostructured silica-surfactant film with time. The film was prepared under TEOS and HCl vapors at 120 °C.

### Results and Discussion

**Formation of Mesostructured Films under TEOS and HCl Vapor.** Figure 2(a) shows the time-course of the XRD pattern of a silicate-surfactant film under TEOS and HCl vapor at 120 °C. The change in  $d(100)$  spacing with time is also shown in Figure 2(b). The XRD pattern of as-coated surfactant film (0 min) has two reflection peaks which are corresponding to (100) and (200) peaks. The  $d(100)$  was calculated to be 2.6 nm which is roughly twice as long as surfactant molecules (CTAB). The surfactant molecules are thought to arrange with a lamellar symmetry. Hydrophobic tails of the surfactant molecules might face the surface of the silicon substrate which has relatively hydrophobic characteristics.

After 15 min, a new peak appeared at 2.5 degree of  $2\theta$ . A gradual increase in this peak with time strongly suggests that TEOS molecules successively penetrated into the interlayer of surfactant molecules and expanded the distance between surfactant layers. The (200) reflection peaks finally disappeared after 60 min implying that nano-phase transition into hexagonal phase of silicate-surfactant nanocomposite occurred under vapor infiltration. The absence of the (110) reflection indicates that the (100) family of planes of the hexagonal unit cell is oriented parallel to the surface of the silicon substrate.<sup>17</sup>

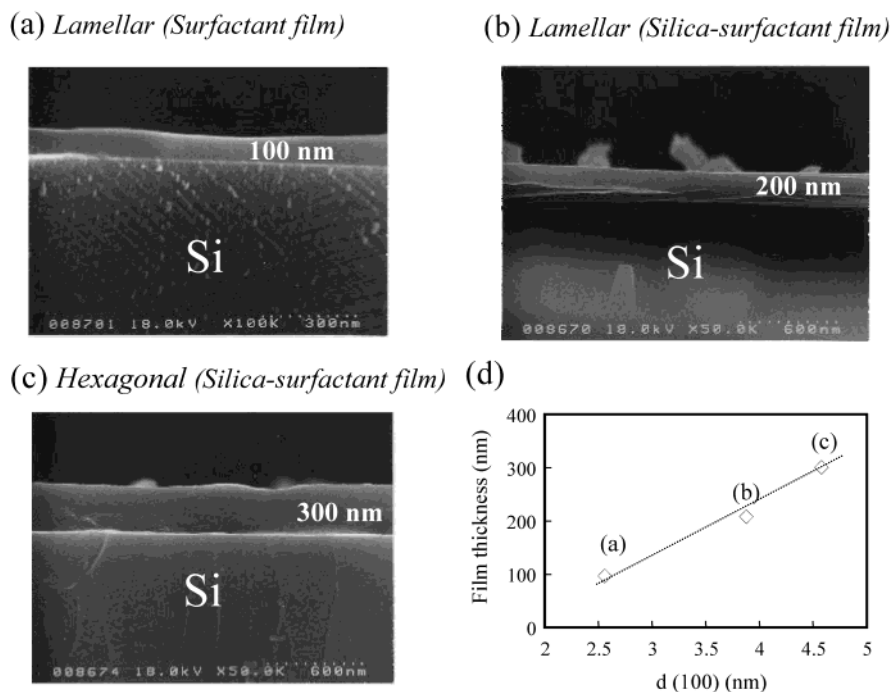


**Figure 3.** FE-SEM images of the cross-section of mesostructured silica films prepared under TEOS and HCl vapors at 120 °C for 2 h. Change in the film thickness of mesostructured silica films with time. The film thickness was plotted as a function of the  $d(100)$  spacing.

According to the increase in the  $d$  spacing by the penetration of TEOS molecules into the films, film thickness should increase with time under vapor infiltration. Figure 3(a)–(c) shows FE-SEM images of the cross-section of mesoporous silica films as well as an originally deposited surfactant film. Continuous and flat mesoporous silica films about 200–300 nm thick were grown from the silicon substrate. There existed no silica particles on the silica film. The features visible on the films are shards of silicate films that are artifacts of the film sectioning. Change in film thickness was plotted as a function of  $d(100)$  spacing in Figure 3(d). The film thickness increased with increasing the  $d(100)$  spacing. This strongly suggests that a swelling in the film thickness is related to a swelling in the distance between layers.

Previously we found that the TEOS molecules can penetrate into spin-on silicate films.<sup>15</sup> In this case, a swelling phenomenon of film thickness ( $d$  spacing) was hardly observed during vapor infiltration. The penetrating TEOS only densified the silica wall to enhance thermal stability of the silica films. This implies that after the formation of silicate network proceeds to some extent, the swelling of film thickness ( $d$  spacing) does not occur further although TEOS can penetrate into silica network to densify silica wall. The nano-phase transition under vapor infiltration contains two competitive processes: (1) the penetration of TEOS or TMOS into the films and (2) the reaction of the silanol group. We consider that the rates of these processes depend on the synthetic temperature, silica sources (TEOS and TMOS), catalysts (HCl and  $\text{NH}_3$ ), and the thickness of surfactant films.

**Temperature Dependence of  $d$  Spacing.** The rates of the two competitive processes depend on the synthetic temperature. The effect of synthetic temperature on the  $d$  spacing of the calcined mesoporous films

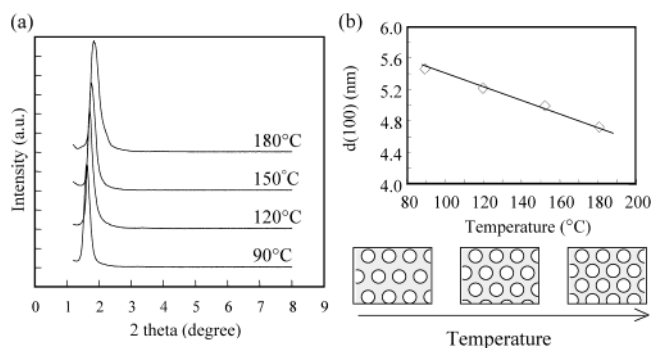


**Figure 4.** (a) XRD patterns of calcined mesoporous silica films synthesized at different temperatures. (b) Effect of synthetic temperature on the  $d(100)$  spacing of mesoporous silica films. Reaction time is 2 h.

is shown in Figure 4. The peak shift of the (100) reflections was not observed after calcination even in the sample synthesized at all the temperatures. The  $d(100)$  spacing of the mesoporous films increases with decreasing synthetic temperature. The reaction rate of condensation of the Si–OH groups strongly depends on the temperature. The rapid formation of a rigid Si–O–Si network at high temperatures stops expansion of  $d$  spacing. On the contrary, at low temperature, a large amount of TEOS molecules can infiltrate into the film before the complete condensation of the Si–OH groups, resulting in the thick silica wall. The  $d$  spacing of the (100) reflection of calcined mesoporous silica films was widely ranged from 3.5 to 5.5 nm, which suggests that the synthetic temperature makes it possible to control the porosity of silica. Further, the porosity can be tuned by changing synthetic conditions such as vapor pressure, film thickness, and silica (TEOS and TMOS) and catalyst (HCl and  $\text{NH}_3$ ) sources, as well as temperature. The examples of these effects will be shown in this paper.

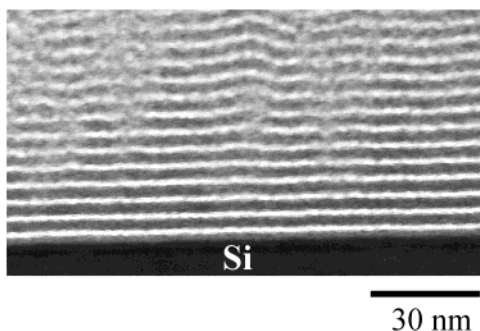


**Figure 5.** STEM images of the cross-sectional view of a calcined mesoporous film on Si substrate. The film was prepared under TEOS and HCl vapor at 120 °C.

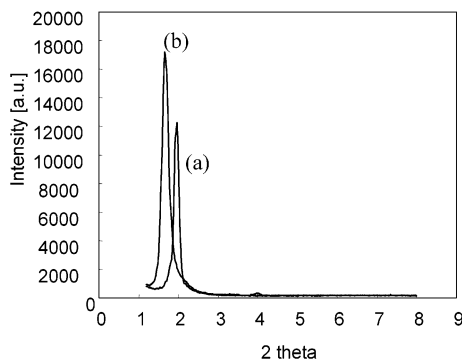


**Figure 6.** XRD patterns of mesoporous silica films prepared under vapors of (a) TMOS and HCl and (b) TEOS and HCl at 120 °C for 60 min.

An STEM image of the cross-sectional views of the calcined film is shown in Figure 5. The films were prepared under TEOS and HCl vapors at 120 °C for 1 h. Ordered straight channels were observed parallel to the surface of the silicon substrate, which is consistent with the results of XRD measurements. The distance from layer to layer is about 5 nm, supporting the  $d(100)$  value shown in Figure 2(b).

**Effect of Reactivity of Vapor Source.** Figure 6 shows the XRD patterns of calcined mesoporous silica films prepared under (a) TMOS and (b) TEOS vapor for 60 min. When TMOS was used as a vapor source, the mesoporous silica film with small  $d(100)$  spacing was obtained. This might arise from the high reactivity of TMOS compared to that of TEOS.

**Film Preparation Using  $\text{NH}_3$  as a Catalyst.** Figure 7 shows the X-ray diffraction (XRD) patterns of (a) a surfactant-deposited silicon substrate, (b) an as-synthesized mesostructured silica film, and (c) a calcined film. The films were prepared under TEOS and  $\text{NH}_3$  vapors at 130 °C for 90 min. Similarly to the results of synthesis using HCl catalyst, no peak shift of the (100) reflection after calcination was observed, indicating that the film preserves the periodic mesostructure without contraction under calcination. This strongly supports that the formed mesostructure on the Si substrate is not a lamellar phase.

The  $d(100)$  spacings of as-synthesized and calcined films prepared using  $\text{NH}_3$  vapor were plotted as a function of synthetic temperature in Figure 8. The  $d$  spacing decreased with increasing temperature, which is the same trend shown in Figure 4. However, the  $d$  spacing of the mesostructured silica films prepared

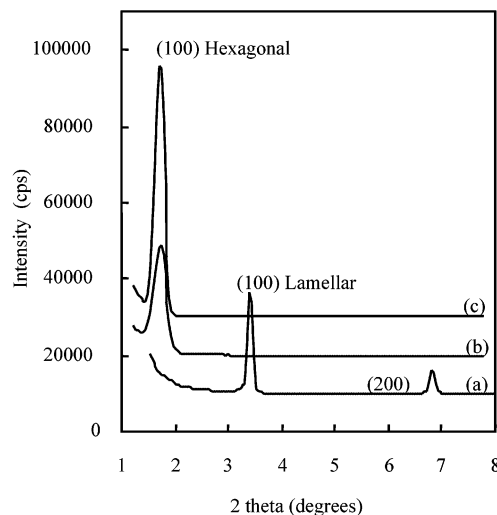


**Figure 7.** XRD patterns of mesostructured silica films. (a) a surfactant film before vapor infiltration, (b) an as-synthesized film, (c) a calcined film. The film was prepared under TEOS and  $\text{NH}_3$  vapors at 130 °C for 90 min.

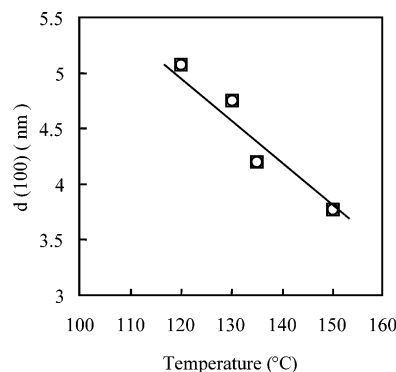


**Figure 8.** Effect of synthetic temperature on the  $d$  spacing of mesostructured silica films.  $\circ$ , as-synthesized films;  $\square$ , calcined films. The films were prepared under TEOS and  $\text{NH}_3$  vapors.

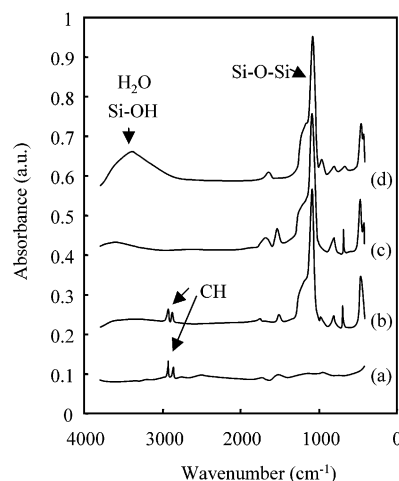


**Figure 9.** FTIR spectra of mesostructured silica films. (a) a layered surfactant film, (b) an as-synthesized film prepared under TEOS and  $\text{NH}_3$  vapors at 135 °C, (c) a calcined film, (d) a calcined mesoporous silica film synthesized by a conventional sol-gel method.

using  $\text{NH}_3$  was smaller than the ones prepared using HCl. This implies that the reaction rate of TEOS is higher under  $\text{NH}_3$  vapor than under HCl. The reaction



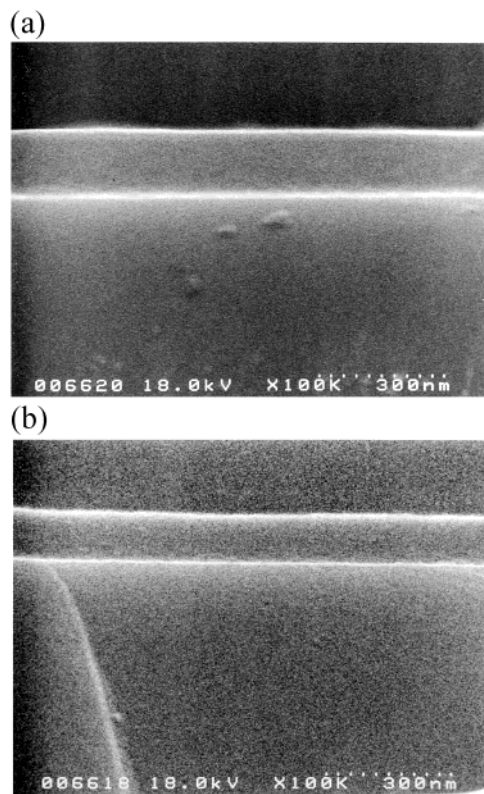


**Figure 10.** FE-SEM images of the cross-section of calcined mesoporous films. Surfactant films were deposited on silicon substrates spinning (a) 4000 rpm and (b) 6000 rpm. The films were prepared under TEOS and  $\text{NH}_3$  vapors at 130 °C.

rate of TEOS can also be controlled by changing the concentration of  $\text{NH}_3$  and HCl solutions.

**Si-OH Groups in Mesoporous Silica Films.** The high structural stability shown in Figure 7 has hardly been attained on the mesoporous silica films synthesized by conventional sol-gel techniques (especially spin-on silicate films).<sup>15</sup> The structural shrinkage seems to be very serious problem especially on supported films. When a film adhering to a substrate shrinks, the entire film is subjected to mechanical stress. This stress may lead to cracking.

The contraction of silica under calcination is associated with the condensation of residual silanol (Si-OH) groups in the wall. The FTIR spectra of mesostructured films prepared under TEOS and  $\text{NH}_3$  vapors at 135 °C are shown in Figure 9. We compared these spectra to

the one obtained by a sol-gel process. The sharp absorption bands at 1100  $\text{cm}^{-1}$  observed in the spectra (b), (c), and (d) are ascribed to the Si-O-Si framework. The broad band observed at about 3500  $\text{cm}^{-1}$  in the spectrum (d) is assigned to the Si-OH groups and adsorbed  $\text{H}_2\text{O}$  on the Si-OH groups. The absence of this broad band in the spectra of the samples synthesized by vapor infiltration shows that the concentration of residual Si-OH groups is extremely low even before calcination. This is the reason the mesostructured films hardly contract during calcination. The vapor infiltration process was conducted at high temperatures in the absence of aqueous solution, which are advantageous synthetic conditions to the complete condensation of the Si-OH groups. The silica wall densified by successive penetration of TEOS molecules has high structural stability and hardly contracts under calcination process.

The pore surface of silica films is thought to be more hydrophobic than the ones by the sol-gel method because of low concentration of the Si-OH groups and the adsorbed  $\text{H}_2\text{O}$ . If the films are used as low- $k$  dielectric film, the low adsorption capacity of water is an attractive feature because the dielectric constant of water is very large ( $k = 81$ ). The calcined films maintained their ordered structure after hydrothermal treatment exposing them to a saturated water vapor at 90 °C for 2 h, showing excellent hydrothermal stability. The band at 2900  $\text{cm}^{-1}$  disappeared in the calcined film, confirming the complete removal of surfactant molecules after calcination at 400 °C.

#### Effect of Film Thickness Of Surfactant Films.

Figure 10 shows FE-SEM images of the cross-sections of calcined mesoporous silica films. The films (a) and (b) were prepared under TEOS and  $\text{NH}_3$  vapors at 130 °C. Surfactant films were deposited on the Si substrate spinning (a) 4000 rpm and (b) 6000 rpm. Continuous and flat mesoporous silica films about (a) 200 nm and (b) 150 nm thick were grown from the silicon substrate. There existed no silica particles on the silica film. The difference in the film thickness is associated with the thickness of originally deposited surfactant films. The surfactant films, which are deposited on the substrate with a high spinning rate, give thinner mesoporous silica films. This result shows that the thickness of mesoporous silica films can be controlled by changing the thickness of surfactant films before the vapor infiltration process.

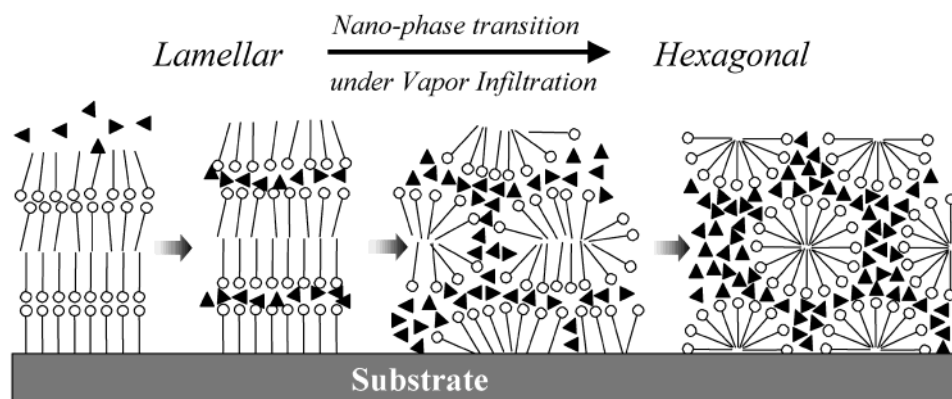


**Figure 11.** Graphical illustration of the proposed model for the formation of a mesoporous silica film on a Si substrate via vapor infiltration.

**Formation of Mesostructured Silica Films.** We proposed a model for the formation of mesostructured film under vapor infiltration as shown in Figure 11. The TEOS molecules infiltrate into a surfactant film on the silicon substrate. The TEOS molecules in the film interact with the hydrophilic headgroups of surfactants and form TEOS–surfactant composites. The TEOS–surfactant composites dynamically rearrange to self-assemble in a hexagonal symmetry (nano-phase transition). Simultaneously, the penetrating TEOS molecules react with the Si–OH groups, resulting in the densification of silica wall.

We found that the nano-phase transition under vapor infiltration occurs not only in the film but also in the powder preparation. After surfactant powder was treated in TEOS vapor, we found that the powder was swelled. The calcined powder shows a hexagonal structure. It seems that the vapor-infiltration method can expand to the synthesis of powder mesoporous materials, which might have physicochemical characteristics different from those of conventional sol–gel products.

## Conclusions

Here we showed a vapor infiltration synthesis for mesoporous silica films with high structural stability. The self-assembling (nano-phase transition) of surfactant–silicate composites under vapor infiltration implies their high mobility in the absence of solvent. This process can be applied to the fabrication of films and powders made of inorganic–surfactant composite materials. This new synthetic method provides opportunities for the creation of new materials technologies.

**Acknowledgment.** This work was supported by the New Energy and Industrial Technology Development Organization (NEDO) under Millennium Research for Advanced Information Technology (MIRAI) project. We thank GHAS laboratory and M. Kawashima (Osaka University) for FE-SEM measurements. We also thank S. Kanemaru and H. Yamauchi (AIST, Tsukuba) for STEM measurements.

CM021011P